**Annales
Geophysicae**

Characteristics of VLF atmospherics near the resonance frequency of the Earth-ionosphere waveguide 1.6–2.3 kHz by observations in the auroral region

A. A. Ostapenko[1], E. E. Titova[1,2], A. P. Nickolaenko[3], T. Turunen[4], J. Manninen[4], and T. Raita[4]

[1]Polar Geophysical Institute, Kola Scientific Centre of Russian Academy of Sciences, Apatity 184200, Russia
[2]Space Research Institute, Russian Academy of Sciences, Profsoyuznaya str, 84/32, 117997, Moscow, Russia
[3]Usikov Institute for Radio-Physics and Electronics, Nat. Acad. of Sciences of the Ukraine, 12, Acad. Proskura street, Kharkov 61085, Ukraine
[4]Sodankylä Geophysical Observatory, Tähteläntie 62, 99600 Sodankylä, Finland

Abstract. Recordings of ELF-VLF waves with the right-hand (RH) and the left-hand (LH) circular polarization were made in Northern Finland. Analysis showed a difference between the RH and LH polarized waves. A pronounced maximum of the wave amplitude was observed at the first critical frequency of the Earth-ionosphere waveguide (the first transverse resonance) around 1.6–2.3 kHz. The wave had the circular LH polarization at this maximum. To interpret observations, we computed the characteristics of the waveguide modes by using the full wave solution in the night model of the ionosphere. Computations show that the spectral maximum at the first transverse resonance frequency arises from a small absorption of the LH polarized radio wave in the magnetized ionosphere plasma, forming the upper boundary of the Earth-ionosphere waveguide.

Keywords. Radio science (Radio wave propagation)

1 Introduction

Measurement of atmospherics (or sferics) is the most straightforward way to study the ELF-VLF radio propagation in the Earth-ionosphere cavity. Signals originate from the lightning discharges and propagate over distances of a few thousand kilometres owing to relatively small attenuation. The sferics carry valuable information about the ionosphere along the propagation path. The idea of using the ELF-VLF natural pulsed radio signals to study the ionosphere and

the lightning strokes was addressed in many works (see e.g. Hayakawa et al., 1994, 1995; Rafalsky et al., 1995; Cummer, 1997, and references therein).

A cavity formed by conducting the earth and the lower ionosphere is a natural electromagnetic resonator (Nickolaenko and Hayakawa, 2002). Sferics are natural radio signals that cover a wide frequency band from a few Hz to tens of kHz. They offer a unique opportunity to investigate the Earth-ionosphere cavity in this frequency band.

Signals of the global electromagnetic resonance occupy the lower ELF band (Schumann, 1952). Transverse resonance of the Earth-ionosphere cavity is observed at ELF-VLF frequencies which is well documented and interpreted (e.g. Rafalsky et al., 1995). The transverse resonance frequencies are $f_p = p\frac{c}{2h}$, where p=1, 2, … is the resonance mode number, h is the effective height of the ionosphere and c is the light velocity. By assuming that h=65–95 km, one obtains the basic resonance frequency $f_1 \in [2.3–1.6]$ kHz (see e.g. Nickolaenko and Hayakawa, 2002). Special observations of transverse resonance were reported in a few works (Belyaev, 1991; Lazebnyi et al., 1988; Rafalsky et al., 1995; Shvets, 1997; Shvets and Hayakawa, 1998; Brundel et al., 2002; Shvets, 2008). Significant maxima of the power spectra were found at multiples of the frequency ~2 kHz at the middle and low latitudes. At high latitude, the experiments on the ionospheric demodulation of the powerful HF radio signal also showed maxima around these frequencies (Stubbe et al., 1982). The measurements showed characteristic low frequency amplitude patterns caused by changes in modulation frequency. The transverse resonance occurs when the standing waves appear between the ground and the ionosphere. In radio propagation, these frequencies are

Correspondence to: E. E. Titova
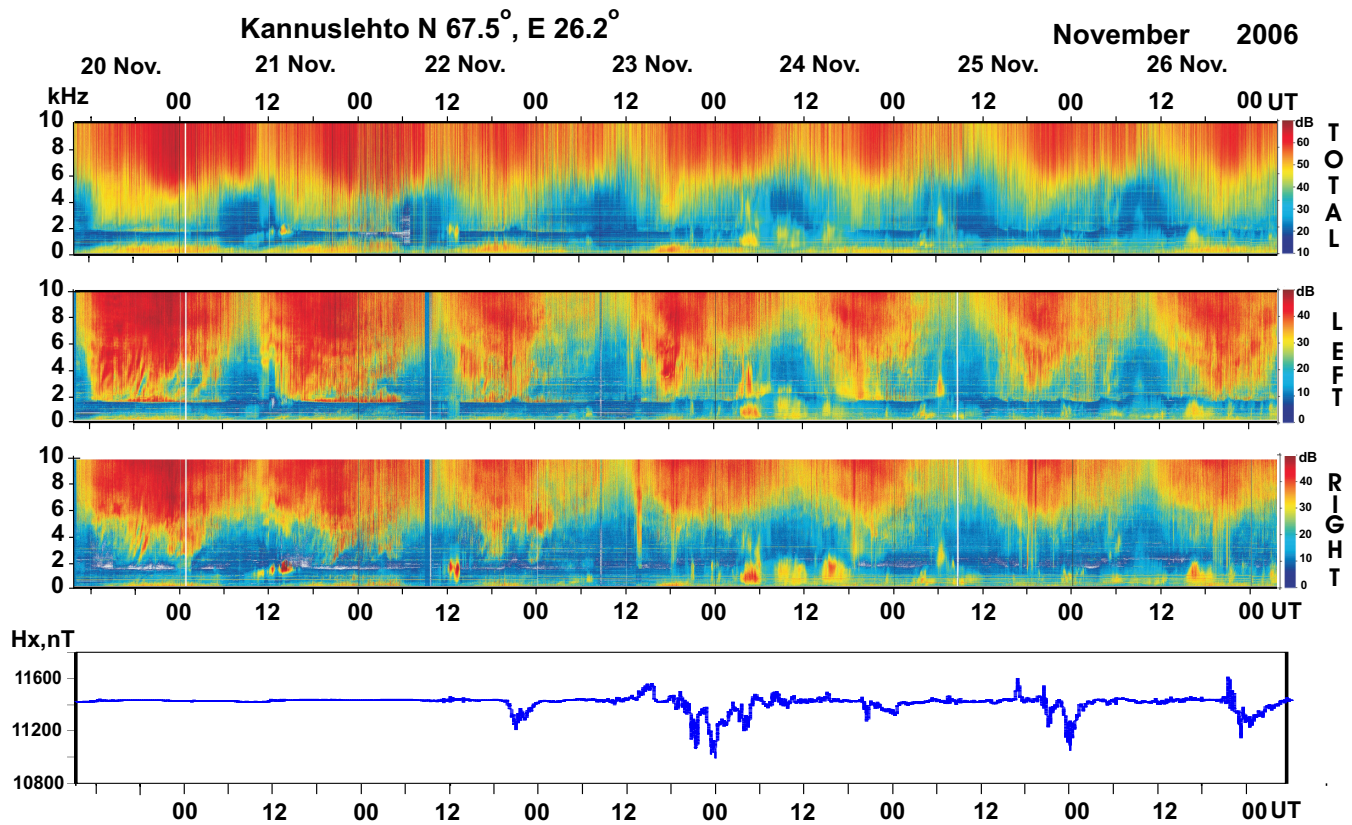(lena.titova@gmail.com)

Fig. 1. Sample spectrograms of ELF-VLF waves recorded during the 20–26 November 2006 campaign in the auroral zone. The upper panel shows the spectrogram of the total power, the second panel represents the dynamic spectrum of the LHP, the third panel depicts the RHP dynamic power spectrum and the bottom plot shows variations of the H_x component of the geomagnetic field at the Sodankula observatory. A narrow band maximum is clearly seen around the first critical frequency of the Earth-ionosphere duct or at the first transverse resonance frequency: around 1.6–1.8 kHz.

regarded as the "cut-off" or critical frequencies of the Earth-ionosphere waveguide.

The "tweek" pulsed radio signals contain specific signatures of transverse resonance in their amplitude spectra (Ryabov, 1992, 1994; Yedemsky et al., 1992; Rafalsky et al., 1995). The tail of a tweek arriving from a remote stroke usually carries a single (the basic) transverse resonance frequency, and its amplitude spectrum has a sharp maximum around 1.6 kHz (Mikhaylova, 1988). Theoretical results (Ryabov, 1992, 1994; Smirnov and Ostapenko, 1986) show that peculiarities must be present in the wave polarization at the eigenmodes of the Earth-ionosphere waveguide, which depend on the ionosphere height and plasma anisotropy. The latter is characterised by the ratio $s=\nu/\omega_H$, where ν is the electron-neutral collision frequency and ω_H is the electron gyrofrequency. The ionospheric gyrotropy becomes significant when $s \ll 1$, i.e., in ambient night conditions when the boundary of lower ionosphere rises to the 85–95 km altitude. Here, the magnetized ionospheric plasma becomes transparent for the right-hand polarized (RHP) waves, while the left-hand polarized waves (LHP) are strongly reflected from the

plasma. This is why the tweek radio signals are observed exclusively during night and are left-handed (Yedemsky et al., 1992; Hayakawa et al., 1994, 1995). The alteration of the wave polarization from the tweek head to its tail was reported by Shvets and Hayakawa (1998).

Yamashita (1977) investigated the long-distance sub-ionospheric propagation in the presence of an anisotropic homogeneous ionosphere. The numerical computations showed a decrease in the attenuation rate at frequencies just above the first cut-off frequency of the Earth-ionosphere waveguide. These results were applied to explain experimental observations of a sharp maximum in the amplitude spectra of the tweek.

In this paper, we present the experimental amplitude and polarization spectra of natural radio signals at frequencies around the first transverse resonance of the Earth-ionosphere cavity (1.6–2.3 kHz). Observations were made at the auroral latitudes (Northern Finland). We also performed the model computations and compare numerical data with observations.
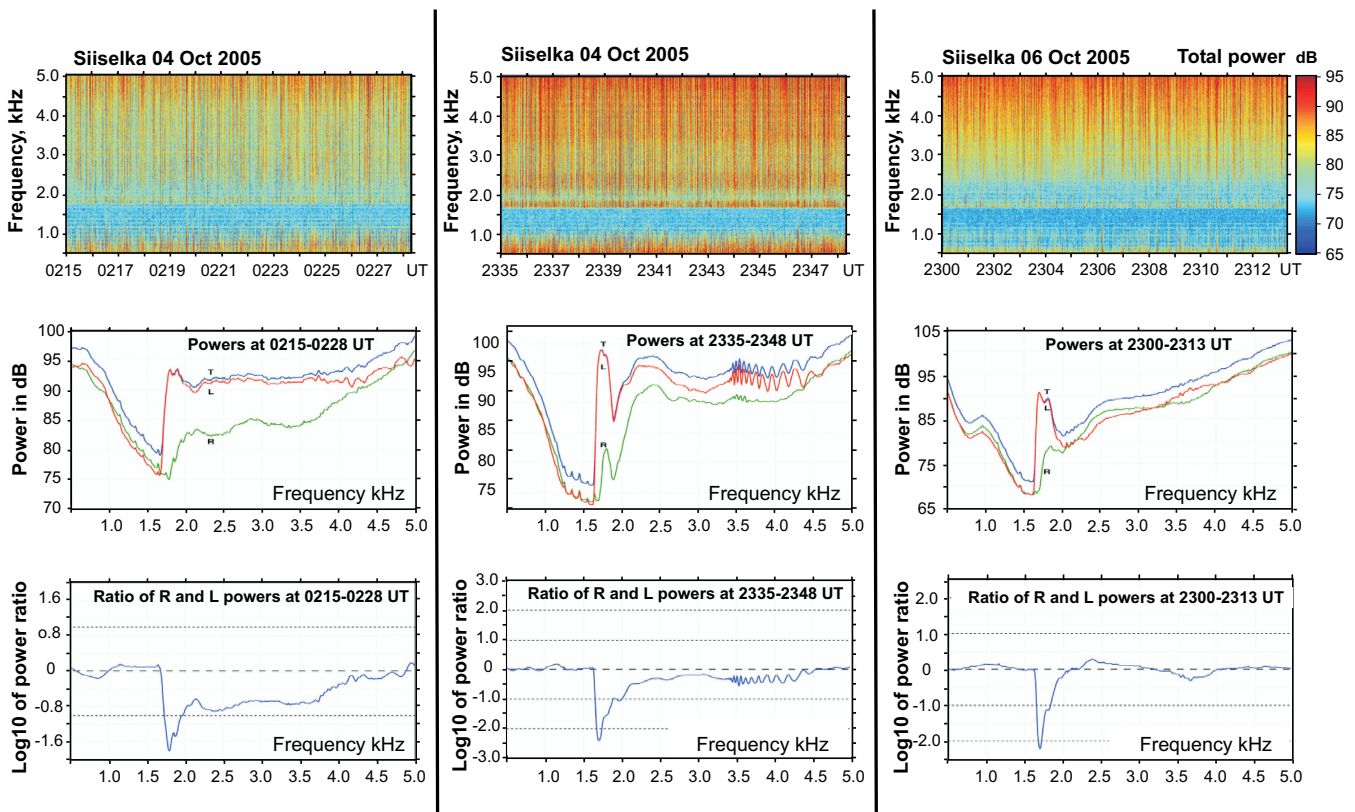
Fig. 2. Typical night-time sferics recorded at the Siselka station during the September–October 2005 campaign. Upper panels show the spectrograms of the total ELF-VLF power at frequencies below 5 kHz. Middle panels depict the power spectra integrated over 13 min< each of them corresponds to the spectrograms shown by the upper panels. The letters T, L, and R denote the total (blue), the LHP (red), and the RHP (green) power spectra. Bottom plots show the ratio of the LHP to the RHP power. At the Earth-ionosphere waveguide cut-off and just above (1.6–1.8 kHz), the perfect left-hand circular polarization prevails.

2 Experimental data

The observations of broadband ELF-VLF radio waves were made in Northern Finland during the measurement campaigns during 2005–2008 (Siiselkä: September–October 2005, Kannuslehto: November 2006, October 2007 and February–March 2008). Continuous recordings cover altogether 45 days. Some recordings were made during the Finnish EISCAT campaigns. The ELF-VLF waveforms were digitally sampled by the 24-bit ADC system and were recorded by the computer together with the GPS timing. The sampling rate was increased from 39.0625 kHz to 78.125 kHz after the 2005 campaign. Two vertical square loop antennas (3 m×3 m) were used during Siiselkä 2005 campaign (geographic coordinates 67.82° N, 26.08° E, L=5.47). The effective area of the antenna was 2300 m^2, and the receiver is known as the "UEV2300 system". The loops were oriented along the magnetic North-South (NS) and the East-West (EW) directions.

During the campaigns in 2006–2008 at Kannuslehto (geographic coordinates 67.74° N, 26.27° E, L=5.46), the antennas were 10 m×10 m coaxial cable loops with 10 turns, hav-

ing the effective area of 1000 m^2. This receiver is known as "VLF100aT". Since 2007, the loops were oriented along the geographical North-South and East-West directions. Accuracy of orientation was based on the theodolite measurements within ±10 arcsec.

Both the observation sites Siiselkä and Kannuslehto are located more than 35 km from the nearest power lines and settlements. The sensitivity of the UEV2300 system is about 1 fT at the 5 kHz, while the VLF100aT receiver reaches the level of 100 aT (0.1 fT). Thus, the receiver noise level is below the natural electromagnetic signal. A detailed description of the Siiselkä 2005 experiment and the data analysis is given by Manninen (2005).

Figure 1 presents the dynamic ELF-VLF spectra for 20–27 November 2006: the dynamic spectra of the total power, LHP power and RHP power. The wideband spectra of the 0–10 kHz band shows a systematic diurnal variation. The maximum intensity is observed around local midnight. Intensity dramatically reduces by noon due to the daytime radio wave absorption in the D-region. The lowest plot in Fig. 1 presents the geomagnetic field variations at Sodankyla Geophysical
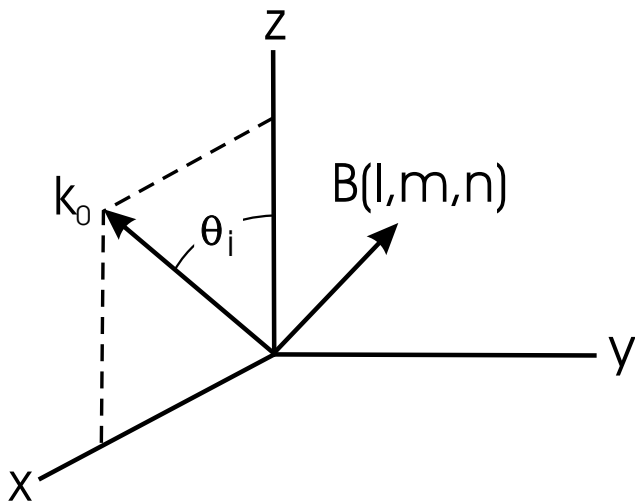
Fig. 3. The coordinate system used in computations. The plane of incidence is the x-z plane. The geomagnetic field $\boldsymbol{B}$ is directed along the (l,m,n) vector.

Observatory. The most disturbed period during the campaign occurred during 22 to 23 November, when the intensity of the sferics decreased. The zero-order mode propagating in the Earth-ionosphere waveguide is seen in Fig. 1 as strong signals below the cut-off frequency of the first transverse resonance mode, around 1.7 kHz.

Figure 1 demonstrates different behaviours of the RH and LH circular polarizations. LHP power exceeds RHP power at frequencies from the cut-off to about 4–5 kHz. Near the first transverse resonance (1.6–2.3 kHz) a narrow maximum is observed in the LHP power during the ambient night condition. Relevant maximum is absent in the RHP power.

Typical nighttime electromagnetic activity is shown in Fig. 2, recorded at Siiselkä. The top panels present the wideband dynamic spectra, the middle panels depict the power spectra integrated over the 13 min (from left to right): 02:15–02:28 UT, 23:35–23:48 UT and 23:00–23:13 UT. The bottom panels show the ratio between the RHP and the LHP powers. The letters T, L, and R in the middle plots correspond to the averaged spectrum of total power (blue curve), the LHP (red curve) and the RHP power (green curve).

Figure 2 shows that the maximum power is observed around the critical frequency of the Earth-ionosphere waveguide (1.6–1.8 kHz) combined with the left-hand circular polarization. It is seen, at the bottom, that the LHP power exceeds the RHP power by two orders of magnitude at transverse resonance. Characteristic oscillations are observed in the spectra at 23:35–23:48 UT around 3 kHz, which might indicate the interference between the first and the second waveguide modes (see Rafalsky et al., 1995).
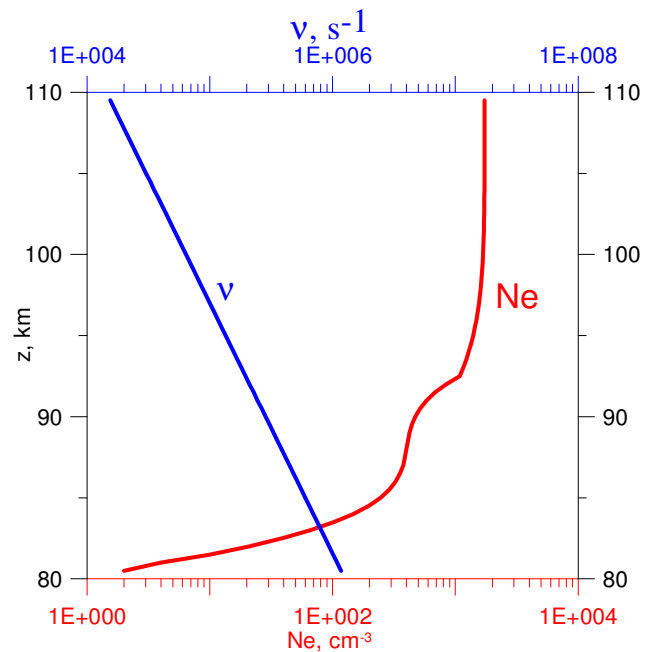

Fig. 4. The electron density and the collision frequency profiles in the night IRI model used in the numerical computations.

3 Computation of electromagnetic field

We derive the characteristics of the low frequency radio waves by using the full wave solution technique given by Budden (1961) (see also Nagano at al., 1975). A Cartesian coordinate system (x, y, z) is used as shown in Fig. 3. A plane wave occurs on an anisotropic medium which is assumed to vary only in the z-direction. The incidence occurs in the X-Z plane. The ionosphere varies along the z-direction only. The orientation of the Earth's magnetic field $\boldsymbol{B}$ is (l,m,n). We assume the time dependence of exp($-i\omega t$) form. The detailed description of the solution is given in Appendix A.

4 Ionosphere model

We used the nighttime IRI model corresponding to geomagnetic latitude 65° and to November 2006. Figure 4 shows the nighttime profile of electron density together with the profile of collision frequency. This particular model corresponds to 20:00 UT, or to 22:00 LT. The altitude z is shown along the vertical axis similar as in Fig. 3. The red curve shows the electron density profile and the corresponding values of electron density are given on the lower horizontal axis. The blue line depicts the profile of electron collision frequency and the relevant values are presented along the upper abscissa. The topside boundary of the ionosphere is assumed to be located at z_u=110 km altitude and the lower ionosphere – neutral atmosphere interface is assumed to be at 80 km altitude.
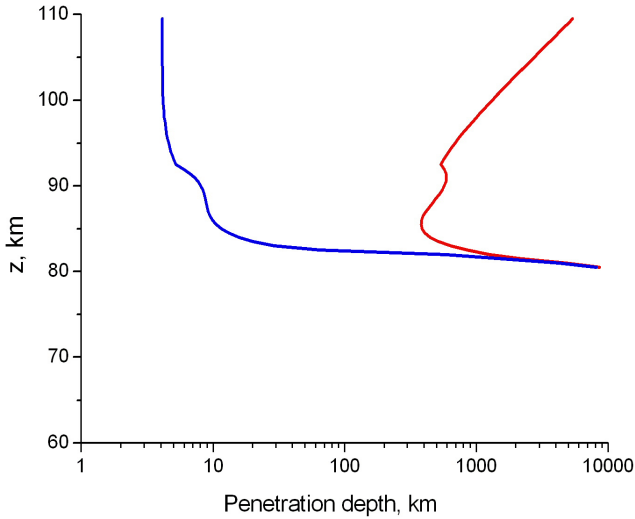
Fig. 5. The penetration depth of the RHP waves (red curve) and of the LHP waves (blue line) at 1600 Hz frequency during the night-time.

5 Estimates of scale depth

During the night, we observe the resonance at a frequency of about 1.6 kHz (see Fig. 2). Hence, the effective height of the ionosphere is $\frac{\lambda}{2} = \frac{c}{2 \cdot f} \approx 94$ km. At this altitude, electron density and collision frequency are $N_e = 1.29 \times 10^3$ cm^{-3}, and $\nu = 1.57 \times 10^4$ s^{-1}, respectively. Relevant refractive indices are $n_L = 0.05 + 6.3 \cdot i$ for the LHP and $n_R = 6.4 + 0.05 \cdot i$ for the RHP wave in the magnetized plasma at 65° geomagnetic latitude. The LHP field amplitude varies as $\exp(i k_0 n_L z) = \exp(-0.23 \cdot z)$. Hence, the scale height of this wave is equal to $\zeta = 1/0.23 = 4.4$ km.

We will regard below the scale height as "scale depth". Figure 5 shows the scale depth of the 1.6 kHz wave as the function of altitude. The red curve corresponds to the RHP wave and the blue line shows LHP wave in the ambient night conditions. It is clear that at 94 km, which correspond to the first transverse resonance frequency, the scale depths are 618 and 4.89 km for the RHP and LHP waves, respectively. The values depart by a factor of 130. This data indicate that the LHP waves are effectively reflected from the ionosphere, while the RHP waves have a large "scale depth" and are poorly reflected. In other words, the great "scale depth" allows the RHP waves to escape into the magnetosphere through the ionosphere.

6 Waveguide modes in the night ionosphere model

The roots of dispersion equation (A5) are the eigenvalues of the waveguide modes and their imaginary part determines the wave attenuation. The tangential electric field is equal to zero at the ground surface and the horizontal magnetic field reaches the maximum here. The wave polarization at the ground surface is defined as:

$$H_R = H_x + i \cdot H_y, \quad H_L = H_x - i \cdot H_y, \quad R = |H_R|,$$
$$L = |H_L|, \quad \varepsilon = \frac{R - L}{R + L} \tag{1}$$

We use the ellipticity parameter ε, which is $+1$ for the circular RHP wave and -1 for the circular LHP. In the general case, the sign of ε gives the sense (direction) of rotation of the field vector. Parameter ε is positive for the RHP waves (i.e. the counter-clockwise rotation when the wave propagates along the Earth's magnetic field) and it is negative for the LHP waves.

Figure 6a shows attenuation coefficients for the first 5 modes in the frequency range of 1–4 kHz computed from Eq. (A13). The modes are labelled in accordance to the right (R) or the left (L) polarizations; the numbers denote the mode number. One may notice in Fig. 6a that the first-order and the second-order waveguide modes start to propagate from frequencies of 1.6 and 3.2 kHz. The "new-born" waves have initially a large attenuation factor (at frequencies just above the cut-off). The attenuation rapidly decreases with frequency and soon it reaches the level of the conventional losses in the Earth-ionosphere duct. It is also obvious that the attenuation factor of the LHP waves is smaller than that of the RHP waves at all frequencies.

The real part of the longitudinal or the x-component of the refraction index $n_x = k_x/k_0$ is shown in Fig. 6b. It is related to the phase velocity V_{ph} by the formula Re $(n_x) = c/V_{ph}$. The zero-order modes of the waveguide L0 and R0 satisfy the relation:

$$n^2 = n_x^2 + n_z^2; \quad n_x = 1; \quad n_z = 0. \tag{2}$$

The wave number at the transverse resonance satisfies the condition:

$$k_z = \frac{2\pi}{\lambda_z} = \frac{\pi}{h}; \quad k_x = \sqrt{k_0^2 - k_z^2};$$
$$n_x = \frac{k_x}{k_0} = \sqrt{1 - \frac{\pi^2}{(k_0 h)^2}}. \tag{3}$$

As it can be seen in Fig. 6b, the refraction index Re $(n_x) \approx 1$ for the zero-order modes L0, R0, hence, these are the propagating modes. The zero-order mode TH0, which is also regarded as the E0-wave, does not have the lower cut-off frequency. This mode supports the long distance ELF propagation at frequencies below the first transverse resonance frequency (e.g. Kikuchi and Araki, 1979; Nickolaenko and Hayakawa, 2002).

Frequency dependence of the L1 mode indicates its capture by the waveguide at the frequency of the first transverse resonance. The refraction index n_x of this mode is equal to zero at the resonance frequency and it grows towards 1 with the frequency increase. Electromagnetic energy of the
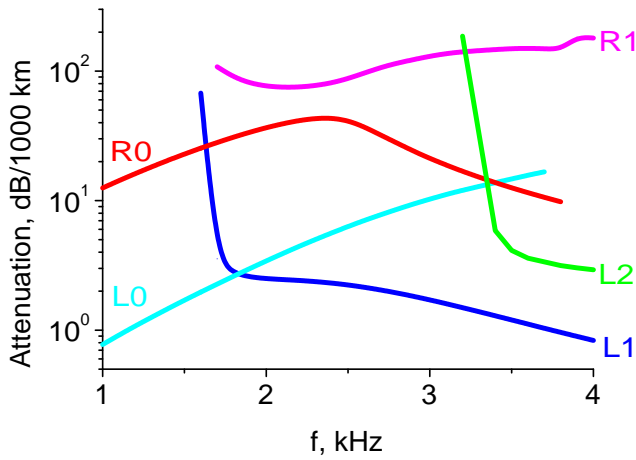
Fig. 6a. Attenuation factor of different modes for the night IRI model of ionosphere.
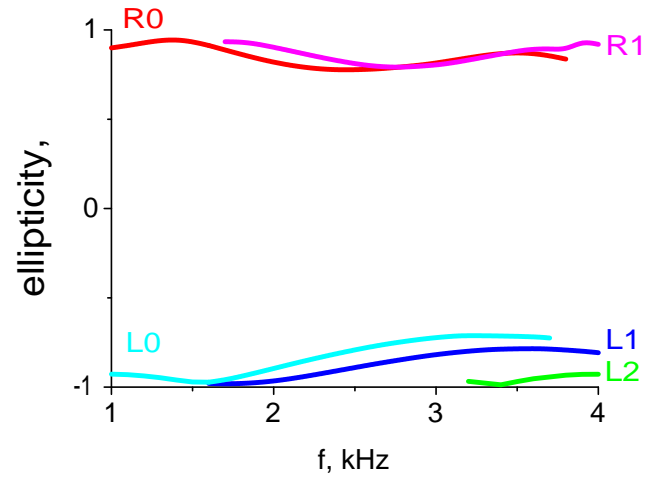

Fig. 6b. X-component of refraction index for different modes.

Fig. 6c. Polarization of different modes for the night IRI model of ionosphere.

Polarization ellipticity ε is shown in Fig. 6c for different eigenmodes. One can see that LHP wave has the circular polarization at resonance frequencies, as $\varepsilon \approx -1$ here. The LHP have the lowest attenuation rate above the resonance frequency. This conclusion is confirmed by observations: the left-hand polarized waves dominate at frequencies above the first transverse resonance.

The field amplitude reaches its maximum at the resonance frequency in conventional resonance phenomena. One could expect a similar maximum in the amplitude spectrum of transverse resonance, as it was observed in experiments with the HF powerful transmitter of modulated amplitude (Stubbe, 1982). However, computations predict a large attenuation factor at the resonance frequency (Fig. 6a), so that radio waves cannot propagate effectively in the Earth-ionosphere duct. Two questions arise. In what way does the narrow maximum appear in the amplitude spectrum of the distant sferics? Does its position depend on the distance between the source and observer?

7   Transverse resonance spectra excited by in-phase planar current

We computed amplitude spectra excited by the in-phase planar current placed below the nighttime ionosphere. The selection of the horizontal source current is justified by the following reason. The transverse resonance is associated with radio waves trapped between the ground and the lower ionosphere (Lazebny et al., 1988; Rafalsky et al., 1995; Hayakawa et al., 1994, 1995; Nickolaenko and Hayakawa, 2002). Such waves propagate vertically; hence, only horizontal current might be an effective source of the transverse resonance. In the case where the causative lightning discharge has a tilted channel, the horizontal projection of its

first waveguide mode is "trapped" at the first transverse resonance frequency. Indeed, according to the modal equation $k^2 = k_x^2 + k_z^2$, we obtain $k_x = 0$ in this case as $1 - (k_z)^2 = 0$ at the particular resonance frequency of $f_1 = \frac{c}{2h}$. Physically, the phase front of the trapped radio wave is horizontal, parallel to the boundaries. This wave is the standing wave. Owing to the particular frequency, nothing is left in the dispersion relation for a non-zero k_x component responsible for the horizontal propagation. Therefore, the wave is captured at $f = f_1$ and the Earth-ionosphere cavity acts as a planar Fabry-Perot resonator. All the sites at the ground surface will detect the radio wave with the zero mutual phase shift. A non-zero k_x component appears at higher frequencies and the first-order waveguide mode starts to propagate horizontally. The phase delay appears with the frequency increase, which depends on the length of the propagation path. This phase shift was exploited for establishing the source-observer distance (Rafalsky et al., 1995; Brundel et al., 2002). Finally, the wave front turns into a vertical plane at the infinite frequency.

current serves as the field source for the transverse resonance signals.

We use an infinite horizontal in-phase current sheet as the source, which is positioned at the height of lightning discharges z=7 km. The horizontal planar current J_{ext} flows in the Y-direction, so that only the B_x component is present. The amplitude of the current is independent of frequency: J_{ext}=const. Results of field computations are presented in Fig. 7, where the source frequency is shown along the abscissa in kHz and the amplitude $|B_x|$ is depicted along the ordinate in arbitrary units. Our idealized source model allows obtaining the transverse resonance in the clearest fashion, demonstrated by Fig. 7.

The spectrum of Fig. 7 contains pronounced peaks corresponding to two transverse resonance modes. The signal amplitude is increased by an order of magnitude owing to the resonance. Amplitude of the second transverse resonance mode exceeds that of the basic mode. It is explained by the growing efficiency of horizontal source when the frequency increases.

Thus, in the vicinity of horizontal lightning discharge, one can expect the amplitude maximum to be elevated over the "podium" by an order of magnitude. In the case of our observations, the major sources were located at distances of a few thousands kilometres.

Figure 6 shows the wave attenuation factor exceeding 20 dB per 1000 km at frequencies above the transverse resonance. Such attenuation would compensate the excess of the resonance amplitude, provided that the distance from the source to observer is 1000 km or more. Therefore, the experimental maximum seen in Fig. 1 could hardly be associated with the sub-ionospheric propagation: the field sources were a few thousand of kilometres away from the receiver. This is why we believe that regularly observed nocturnal spectral maximum at 1.6–2.3 kHz frequency is connected with the local sources in the auroral zone.

We now consider the ratio R_P of the quality factors pertinent to the LHP and RHP oscillations. It is the inverted ratio of the relevant attenuation rates: $R_P = Q_L/Q_R = \text{Im}\omega_R/\text{Im}\omega_L$. As seen in Fig. 6, the attenuation factor of the LHP waves is two orders of magnitude smaller than that of the RHP wave. This point explains why the LHP waves prevail in the observed resonance maxima, or in the "tail" of tweek atmospherics detected on the ground. The ionosphere is a rather good reflector for the LHP waves. Simultaneously, the RHP waves easily penetrate into the ionosphere and escape from the Earth-ionosphere cavity into the magnetosphere. The idea also explains the origin of "striped" spectral structures of transverse resonance detected on board the DEMETER and other satellites (Ferencz et al., 2007).
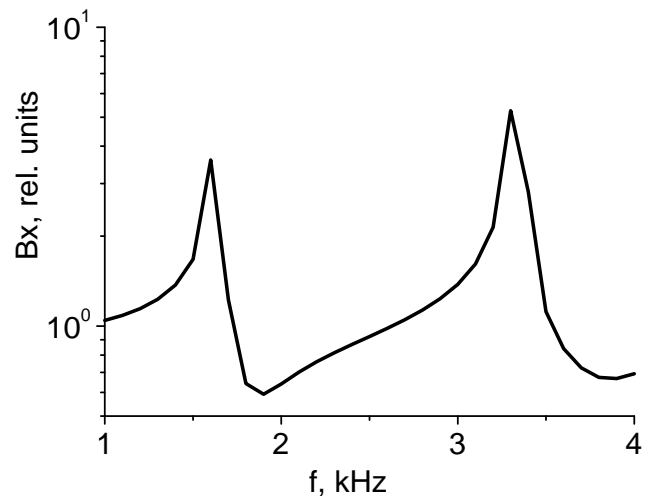

Fig. 7. Amplitude spectra of transverse resonance of the Earth-ionosphere cavity when excited by the infinite planar in-phase current placed at the 7 km altitude above the ground in the ambient night conditions. The amplitude maxima are observed at transverse resonance frequencies of 1.6 and 3.2 kHz.

8 Discussion

The amplitude and polarization spectra of high latitude sferics are often similar to those observed at the mid-latitudes (Yedemsky et al., 1992; Mikhaylova, 1988) or in the vicinity of the equator (Hayakawa et al., 1994, 1995).

The first-order mode radio wave has the LHP at all frequencies and it acquires the circular LHP at the resonance (or the cut-off) frequency of 1.7–1.8 kHz (Yedemsky et al., 1992; Hayakawa et al., 1994, 1995). Tweek amplitude spectra have the sharp maximum and a strong dispersion nearby this frequency (Mikhaylova, 1988). Hayakawa et al. (1994, 1995) used the full wave solution when modelling tweek polarization in the Earth-ionosphere waveguide with a realistic electron density profile. Our results confirm their conclusion that the attenuation of the first mode LHP wave is much lower than that of the RHP waves. This is the reason why only the LHP waves are observed at frequencies just above the first cut-off frequency of the Earth-ionosphere waveguide.

However, Hayakawa et al. (1994, 1995) do not explain the well-pronounced amplitude maximum present in the spectra of the long distance tweeks: the peak is positioned at the cut-off frequency (Mikhaylova, 1988). The emergence of such a peak was addressed in works by Yamashita (1977) and Ryabov (1992, 1994). They have found that the attenuation factor of the corresponding waveguide mode has a narrow minimum just above the Earth-ionosphere waveguide cut-off. Thus, the minimum of losses is observed as a sharp maximum in the amplitude spectrum of tweeks.

Our computations are based on the full wave solution and the obtained results deviate from those published by Yamashita (1977) and Ryabov (1992): we did not find any

minima in the wave attenuation rate around the transverse resonance (the waveguide cut-off) frequency. Therefore, the maximum in the amplitude spectrum of sferics at the critical frequency of the waveguide must be attributed to the transverse resonance of the Earth-ionosphere duct. Computations performed with the planar current source show a pure spectrum of the transverse electromagnetic resonance, which corresponds to radio waves captured between ground and the ionosphere. Such waves are effectively excited by horizontal currents (e.g. Lasebny et al., 1988; Rafalsky et al., 1995; Nickolaenko and Hayakawa, 2002).

In reality, the remote field source has the finite horizontal dimension. Therefore, the radio propagation is always present in the experiment. Guided radio waves travel in a duct as a number of modes. Different modes interfere and the observed amplitude spectrum becomes substantially modified. A characteristic "mode beating" appears at every frequency of the transverse resonance (Rafalsky et al., 1995; Nickolaenko and Hayakawa, 2002). The clear resonance pattern might be observed only in the spectrograms of distant sferics.

The transverse resonance in its pure form might be observed only for a short distance between the source and observer. Such a situation was realised in the experiments of ionospheric HF heating (Stubbe at al., 1982). Sometimes the transverse resonance is observed in the integrated daytime ELF-VLF power spectra, provided that a thunderstorm occurs close to the receiver (Lazebnyi et al., 1988; Belyaev et al., 1991).

9   Conclusion

We made a study of ELF-VLF sferics recorded in Northern Finland. Sensitive receivers allowed the detection of natural radio waves and relevant polarization studies of the field. Pronounced amplitude maximum was detected near the first transverse resonance frequency of the Earth-ionosphere waveguide ($\sim$1.6 kHz) in night conditions. Received radio waves had the circular LHP, which prevails at frequencies up to 4–5 kHz.

Experimental results are interpreted with the full wave solution for the particular geometry of the nighttime ionosphere. We found that the attenuation factor of the LHP wave is much smaller than that of the RHP wave, which allows the leakage of the RHP wave into the magnetosphere through the anisotropic ionosphere.

Transverse resonance spectra were computed for the field source in the form of a planar infinite horizontal current sheet. Analysis showed that transverse resonance becomes evident when the wave propagates only in the vertical direction. This means that its convincing pattern might be obtained for the nearby sources.

The problem remains in the nearby field source at high latitudes. To resolve this problem one has to treat the ex-

citation efficiency of remote horizontal lightning discharges (the wave propagating in the sub-ionospheric duct) and this one of the signal arriving from the magnetosphere (the waves propagating in plasma along the magnetic field lines).

Appendix A

The full wave solution

We derive the characteristics of the low frequency radio waves by using the technique suggested by Budden (1961) (see also Nagano at al., 1975). A Cartesian coordinate system (x, y, z) is used as shown in Fig. 3. A plane wave is incident on an anisotropic medium from below at an angle θ to the z-axis. The incidence occurs in the X-Z plane. Ionosphere varies along the z-direction only. The orientation of the Earth's magnetic field is (l, m, n). We assume the time dependence of the $\exp(-i\omega t)$ form. Electromagnetic fields satisfy the following Maxwell's equations:

$$\nabla \times \boldsymbol{H} = -i\omega\varepsilon_0(\mathbf{I}+\mathbf{M})\boldsymbol{E} \tag{A1}$$

$$\nabla \times \boldsymbol{E} = i\omega\mu_0\boldsymbol{B} \tag{A2}$$

where ε_0, μ_0 are the free space permittivity and permeability correspondingly, $\mathbf{I}$ denotes the unit matrix, and $\mathbf{M}$ is the susceptibility matrix with the following elements:

$$M_{xx} = -X(U^2 - l^2Y^2)/U(U^2 - Y^2),$$
$$M_{xy} = -X(iUnY - nlY^2)/U(U^2 - Y^2),$$
$$M_{xz} = -X(-iUmY + lmY^2)/U(U^2 - Y^2),$$
$$M_{yx} = X(-iUnY + lrnY^2)/U(U^2 - Y^2),$$
$$M_{yy} = -X(U - m^2Y^2)/U(U^2 - Y^2),$$
$$M_{yz} = -X(iUIY - mnY^2)/U(U^2 - Y^2),$$
$$M_{zx} = -X(iUmY - lnY^2)/U(U^2 - Y^2),$$
$$M_{zy} = X(-iUnY)/U(U^2 - Y^2),$$
$$M_{zx} = -X(U - n^2Y^2)/U(U^2 - Y^2),$$

Here, we apply the following symbols: $U=1+iZ$; $Z=\nu/\omega$; $X=(\omega_p/\omega_H)^2$; $\omega_p^2 = e^2N/m\varepsilon_0$; $\omega_H=eB/m$; $Y=\omega_H/\omega$; ω_p is the plasma circular frequency; ω_H is the electron gyro frequency; m and e are the electron mass and its charge correspondingly; N is the electron density, ν is the electron collision frequency.

The ionosphere is the horizontally stratified medium and the space-time dependence of each field component in the incident wave is proportional to $\exp[-i\omega t + ik_0(n_x x + n_z z)]$, where k_0 is the propagation constant of the free space, $n_x =\sin\theta$, $n_z =\cos\theta$. By eliminating the E_z and H_z components from Eqs. (1) and (2) and by applying the Snell's law, we obtain the following equation (Budden, 1961):

$$d\mathbf{e}/dz = ik_0\mathbf{T}\mathbf{e}, \tag{A3}$$

where $\mathbf{e}$ is the column matrix composed of the horizontal electric and magnetic field components:

$$\mathbf{e} = \begin{bmatrix} E_x \\ E_y \\ Z_0 H_x \\ Z_0 H_y \end{bmatrix}, \quad Z_0 = (\mu_0/\varepsilon_0)^{1/2},$$

and $\mathbf{T}$ is the 4×4 matrix

$$\mathbf{T} = \begin{bmatrix} -\frac{n_x M_{zx}}{1+M_{zz}} & \frac{n_x M_{zy}}{1+M_{zz}} & 0 & \frac{1-n_x^2+M_{zz}}{1+M_{zz}} \\ 0 & 0 & -1 & 0 \\ \frac{M_{yz}M_{zx}}{1+M_{zz}} - M_{yx} & 1 - n_x^2 + M_{yy} - \frac{M_{yz}M_{zy}}{1+M_{zz}} & 0 & \frac{n_x M_{yz}}{1+M_{zz}} \\ 1 + M_{xx} - \frac{M_{xz}M_{zx}}{1+M_{zz}} & \frac{M_{xz}M_{zy}}{1+M_{zz}} - M_{xy} & 0 & -\frac{n_x M_{xz}}{1+M_{zz}} \end{bmatrix}.$$

If the medium is divided into a number of thin homogeneous slabs, formula (A3) becomes a differential equation with a constant matrix $\mathbf{T}$ within each layer. Then, a particular solution of Eq. (A3) corresponds to the factor $\exp(-ik_0 qz)$ combined with the complex wave amplitude. We obtain from Eq. (A3)

$$(\mathbf{T} - q\mathbf{I})\mathbf{e} = 0 \tag{A4}$$

The condition of a nontrivial solution of Eq. (4) is:

$$\mathrm{Det}(\mathbf{T} - q\mathbf{I}) = 0 \tag{A5}$$

Relation (A5) gives the so-called Booker quadric equation for q and the relevant eigen values determine the characteristic modes of upgoing and downgoing waves being each of the LHP and the RHP types. Equation (A5), within a homogeneous layer, provides the eigenvalue q_l and Eq. (A4) allows for constructing the corresponding eigenvectors of the problem.

Let us turn to the solution of the equation with a non-zero right part:

$$\frac{d\mathbf{e}}{dz} - ik_0 \mathbf{T}\mathbf{e} = \mu_0 \mathbf{J}_{\mathrm{ext}}, \tag{A6}$$

where $\mathbf{J}_{\mathrm{ext}}$ is the external source current. The general solution of the fourth-order differential Eq. (A6) has the following form:

$$\mathbf{e} = \sum_{i=1}^{i=4} c_i \cdot \mathbf{e}_i, \tag{A7}$$

Here, the index i denotes solutions (and eigenvalues) relevant to the LHP and RHP waves propagating upward ($i=1, 2$), or to the LHP and RHP waves propagating downward ($i=3, 4$).

Since the WKB approach is valid at the upper boundary of the ionosphere, the reflected waves are absent, and only the waves travelling upward remain:

$$\mathbf{e} = \sum_{i=1}^{i=2} c_i \cdot \mathbf{e}_i \text{ for } z = z_U \tag{A8}$$

In a "straight marching" procedure, the partial solutions $\mathbf{e}_1$ and $\mathbf{e}_2$ are constructed step by step downward starting at the

upper boundary and finishing at the ground surface. The coefficients c_1, c_2 remain undefined. To establish them, a particular solution of inhomogeneous Eq. (A6) $\mathbf{e}_{\mathrm{nh}}$ must be added to the general solution (A8)

$$\mathbf{e} = \sum_{i=1}^{i=2} c_i \cdot \mathbf{e}_i + \mathbf{e}_{\mathrm{nh}} \tag{A9}$$

Combination (A9) must satisfy the boundary conditions on the perfectly conducting surface of the Earth and the unknown coefficients c_1, c_2 are found.

The field discontinuities might be met. For example, a current sheet $\mathbf{J}_{\mathrm{extv}}$ positioned in the ionosphere at the height z_0 causes a discontinuity in the tangential magnetic induction:

$$\{B_x\} \equiv \left(B_{x_2} - B_{x_1}\right)\big|_{z=z_0} = \mu_0 \mathbf{J}_{\mathrm{extv}} \tag{A10}$$

while

$$E_{x_1}\big|_{z=z_0} = E_{x_2}\big|_{z=z_0} = E_{y_1}\big|_{z=z_0} = E_{y_1}\big|_{z=z_0} \tag{A11}$$

or

$$\left\{ \begin{array}{l} c_1 E_{x1} + c_2 E_{x2} + E_{x\mathrm{nh}} = 0 \\ c_1 E_{y1} + c_2 E_{y2} + E_{y\mathrm{nh}} = 0 \end{array} \right\} \tag{A12}$$

The solution of system (A12) is unique when the following condition is satisfied:

$$\begin{vmatrix} E_{x_1}(z_1) \; ; \; E_{y_1}(z_1) \\ E_{x_1}(z_1) \; ; \; E_{y_2}(z_1) \end{vmatrix} \neq 0$$

In the absence of source current $\mathbf{J}_{\mathrm{ext}}=0$ the following dispersion relation is obtained:

$$\begin{vmatrix} E_{x_1}(z_1) \; ; \; E_{y_1}(z_1) \\ E_{x_1}(z_1) \; ; \; E_{y_2}(z_1) \end{vmatrix} = 0 \tag{A13}$$

It defines the complex eigenvalues: the phase velocity of radio waves and the attenuation factor.

References

Belyaev, P. P., Buzunkin, A. A., and Lisov, A. A.: Structure of electromagnetic noise spectra in waveguide Earth-ionosphere at frequency (1–10) kHz., in The low frequency Earth-ionosphere waveguide, Publishing house "Gylym", 90–96, 1991.

Brundell, J. B., Rodger, C. J., and Dowden, R. L.: Validation of single-station lightning location technique, Radio Sci., 37(4), 12-1, 1059, doi:10.1029/2001RS002477, 2002.

Budden, K. G.: Radio waves in the ionosphere, Cambridge University press., 1961.

Cummer, S. A.: Lightning and ionospheric remote sensing using VLF/ELF radio atmospherics, PhD thesis, Dept. of Electrical Engineering, Stanford University, Stanford, USA, 1997.

Felsen, L. B. and Marcuvitz, N.: Radiation and Scattering of Waves, Prentice-Hall, Englewood Cliffs, N.J., 888 p., 1973.

Ferencz, O. E., Ferencz, Cs., Steinbach, P., Lichtenberger, J., Hamar, D., Parrot, M., Lefeuvre, F., and Berthelier, J.-J.: The effect of subionospheric propagation on whistlers recorded by the DEMETER satellite – observation and modelling, Ann. Geophys., 25, 1103–1112, 2007,
http://www.ann-geophys.net/25/1103/2007/.

Hayakawa, M., Ohta, K., and Baba, K.: Wave characteristics of tweek atmospherics deduced from the direction-finding measurement and theoretical interpretation, J. Geophys. Res., 99(05), 10733–10743, 1994.

Hayakawa, M., Ohta, K., Shimakura, S., and Baba, K.: Recent findings on VLF/ELF sferics, J. Atmos. Terr. Phys., 57(5), 467–477, 1995.

Kikuchi, T. and Araki, T.: Horizontal transmission of the polar electric field to the equator, J. Atmos. Terr. Phys., 41, 927–936, 1979.

Lazebnyi, B. V., Nikolaenko, A. P., Rafal'skii, V. A., and Shvets, A. V.: Detection of transverse resonances of the earth-ionosphere cavity in the mean spectrum of VLF atmospherics, Geomagnetism and Aeronomy, 28, 329–330, 1988.

Lysak, R. L.: Generilized model of the Ionospheric Alfvén Resonator, Geophys. Monogr. Ser., 80, 121–128, AGU, Washington, D.C., 1993.

Manninen, J.: Some aspects of ELF-VLF emissions in geophysical research, Publ. 98, Sodankylä Geophys. Obs., Sodankylä, Finland, available at http://www.sgo.fi/Publications/SGO/thesis/ManninenJyrki.pdf), 2005.

Mikhailova, G. A. and Kapustina, O. V.: Finite frequency-time structure of tweek atmospherics and VLF diagnostics of the parameters of the nighttime lower ionosphere, Geomagnetizm i Aeronomia, 28, 1015–1018, 1988.

Nagano, I., Mambo, M., and Hutatsuishi, G.: Numerical computtion of electromagnetic waves in an anisotropic multilayered medium, Radio Sci., 10(6), 611–617, 1975.

Nickolaenko, A. P. and Hayakawa, M.: Resonances in the Earth-ionosphere cavity, Kluwer Academic Publishers, Dordrecht-Boston-London, 380 p., 2002.

Rafalsky, V. A., Nickolaenko, A. P., Shvets, A. V., and Hayakawa, M.: Location of lightning discharges from a single station, J. Geophys. Res., 100(D10), 20829–20838, 1995.

Ryabov, B. S.: Tweek propagation peculiarities in the earth-ionosphere waveguide and low ionosphere parameters, Adv. Space Res., 12(6), 255–258, 1992.

Ryabov, B. S.: Tweek formation peculiarities, Geomagnetism and Aeronomy, English Translation, 34(1), 60–66, 1994.

Schumann, W. O.: On the radiation free self-oscillations of a conducting sphere which is surrounded by an air layer and an ionospheric shell, Zeitschrift und Naturfirschung, 7a, 149–154, 1952 (in German).

Shvets, A. V. and Hayakawa, M.: Polarisation effects for tweek propagation, J. Atmos. Solar-Ter. Phys., 60(4), 461–469, 1998.

Shvets, A. V.: On polarization properties of tweeks, Radio-Physics and Electronics, 2(2), 101–106, 1997.

Shvets, A. V.: ELF-VLF remote sensing of the Earth – ionosphere cavity, Doctor Degree Dissertastion in Phys-Math sciences, Kharkov, IRE, 308 pp., 2008.

Smirnov, V. S. and Ostapenko, A. A.: Transverse resonances of Earth-ionosphere wave guide in auroral region Geomagnetism and Aeronomy, English Translation, 26(2), 253–257, 1986.

Stubbe, P., Kopka, H., and Rietveld, M. T.: ELF and VLF wave generation by modulated HF heating of the current carrying lower ionosphere J. Atmos. Terr. Phys., 44(12), 1123–1135, 1982.

Yamashita, M.: Propagation of tweek atmospherics, J. Atmos. Terr. Phys., 40, 151–156, 1978.

Yedemsky, D. Y., Ryabov, B. S., Shchokotov, Yu. A., and Yarotsky, V. S.: Experimental investigation of the tweek lieid structure, Adv. Space. Res., 12(6), 251–254, 1992.